

Fingertip Force and Contact Position and Orientation Sensor

Yu Sun

Abstract—This paper presents a novel integrated system that is composed of a fingerprint sensor and a force sensor to measure contact position and orientation of the fingertip along with the contact force. The system uses fingerprints from the fingerprint sensor to identify the contact position and orientation with fingerprint features such as core point and ridge orientations. The contact position and orientation are represented in a fingerpad coordinate system for grasping studies. An experiment has been designed to evaluate the proposed system in terms of accuracy and resolution with three subjects. The proposed system can be used in human grasping studies to characterize the fingerpad contact.

I. INTRODUCTION

Roboticians have learned a great deal from studying human grasping as the human hand exhibits some of the most complex human motor skills. Many studies ([22], [12], [5], [9]) have proposed various taxonomies of human grasping. A basic distinction exists between a power grasp, where the goal is to stabilize an object to resist external forces, and a precision grasp, which is an essential skill to manipulate objects including stable grasps on objects, changing the grasps (re-grasp), and maintaining the grasps during tasks.

A preponderance of research has focused on precision grasps and on instrumentation to measure the fingertip forces and position on the object during contact. A rich experimental paradigm for the study of human grasping was devised by Johansson and Westling [10], consisting of parallel force-sensing pads for opposition grasps between the index finger and thumb. This approach has been generalized to add more touch pads to include the middle, ring, or little fingers. In general, instrumented objects are typically created to incorporate miniature 6-axis force/torque sensors at predefined grasp points (e.g., [20], [21], [16], [19]). Special purpose objects were fabricated to incorporate force sensors.

Besides the complex hand postures and forces during grasping, the great variance in which parts of the fingertip contact an object makes the grasping studies even more complex. To understand human dexterity, it is very important to fully study the local mechanical interaction between the fingerpad and an object. Many studies have been carried out to characterize the mechanical response profile in the fingerpad responding to force. Serina et al. [17], and Pawluk and Howe [14] have examined the dynamic force response of the fingerpad to indentors in different sizes and shapes.

With various kinds of force sensors, the fingertip force and the contact points on the object were measured in different experiments by many research teams to study human dexterous grasping and manipulation. Many robot grasp planning

and control algorithms have been developed with inspirations from human grasping studies. Many encouraging results have been achieved. However, more and more researchers have realized the limitation of only including contact force and contact position on the object. Many researchers have sought for a way to measure the contact position on the fingertip to better model and understand more sophisticated grasping behaviors like rolling and regrasping [4].

Commercial tactile sensors such as FingerTPS from Pressure Profile Systems [15] and flexible tactile sensors from Tekscan [23] have been successfully embedded on many robotic fingers to provide rich spatial grasping information for grasping control. However due to their stiffness, those tactile sensors cannot deform along with the human finger tissue to preserve the elastic profile or precisely measure the contact spatial features, which is not ideal to be used to in many human grasping studies as wearable sensors on fingertips. Most studies attach the tactile sensors on the force sensors other than on fingertips, which provides local contact spatial profiles around the contact point rather than the contact position on the fingertip. Recently, a number of flexible tactile sensors have been developed [7], which could be worn on fingertips as a part of a glove or with a thimble setup. However, the glove or thimble setup may measure differently between trials if the tactile sensor is not aligned with the user's fingertip consistently.

This paper presents a novel fingertip force and position/orientation (FFPO) sensor system that uses a regular force/torque sensor to measure fingertip force and a fingerprint sensor mounted on the force/torque sensor to measure contact position and orientation on the fingertip simultaneously. The fingerprint image obtained from the fingerprint sensor is processed and registered to a pre-constructed fingerprint map with fingerprint core point and ridge orientations. The center position of the registered fingerprint on the fingerprint map in the fingerprint coordinate system is defined as the contact position on the fingertip. Since the contact local spatial features are measured from the fingerprint, the obtained contact position and orientation are always consistent between trials.

Fingerprints have been used in Neuroscience literature to characterize the skin deformation level. Westling and Johansson [25] and Birznieks et al. [2] have measured the area of the fingerprint left on a grasping point to indicate the skin deformation related to grasping force. In the study, the fingertip was stained with ink to enable the measurement. In robotics literature, Levesque and Hayward [11] have used fingerprint features to study the stretch and compression of the human fingerpad skin during tactile exploration. Kurita

Yu Sun is with the Department of Computer Science and Engineering, University of South Florida. yusun@cse.usf.edu

et al. [26] were able to infer contact force by observing fingerprint changes at the point of contact through a glass plate by a camera to estimate the incipient slip movement between the fingertip and the glass. From our best knowledge, the approach of using fingerprints to measure contact positions has not been proposed before.

II. SYSTEM SETUPS

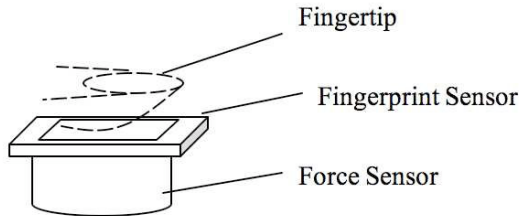


Fig. 1. A schematic drawing of the FFPO sensor system: it is composed of a fingerprint sensor and a force sensor

As illustrated in the schematic drawing Figure 1, the proposed FFPO sensor system is composed of a force sensor and a fingerprint sensor that is rigidly mounted on the top of the force sensor. The center of the fingerprint imaging is aligned with the center of the force sensor, and the short side and the long side of the fingerprint sensor are parallel to the x-axis and the y-axis of the force sensor respectively. The contact force between the user's finger and the FFPO sensor system is measured with the force sensor and the contact spatial properties is characterized with the fingerprint sensor.

Figure 2 and 3 demonstrate two designs with two different types of fingerprint sensors: an optical fingerprint sensor and a solid-state fingerprint sensor. In Figure 2-A, a Futronic FS 90 optical fingerprint sensor (Figure 2-C) is mounted on the tool face of an ATI Nano 17 6-axis force sensor (Figure 2-B). The force readings are collected from a Sensoray 626 data acquisition board and sampled at 1000 Hz. The Futronic FS 90 fingerprint sensor is connected to a PC with a USB cable. The fingerprint image is taken at 10 frame-per-second (fps). The fingerprint sensor has a scanning window size 15x22 mm and image resolution is 440x300 pixel. Its weight is 60 grams with the size of 43(L) x 24(W) x 25(H) mm. It uses infrared LEDs to illuminate the fingertip.

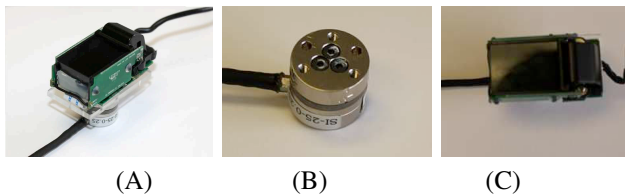


Fig. 2. (A) One design of the proposed integrated system FFPO sensor system that is composed with an ATI Nano 17 force sensor (B) and a Futronic FS 90 optical fingerprint sensor (C).

In Figure 3-A, a solid-state TouchChip TCS1C Fingerprint Sensor (Figure 3-B) is used. It is connected to a TI C5515

Fingerprint Development Kit and connected to the PC with a USB cable. The fingerprint image is collected at 14 fps. The fingerprint sensor has a scanning window size 12.8x18 mm and image resolution is 256 x 360 pixel. The fingerprint sensor has weight at 6 grams with the size of 20.4(L) x 27(W) x 3.5(H) mm [24].

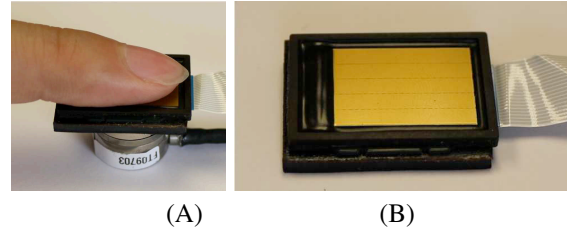


Fig. 3. (A) The second design of the proposed integrated FFPO sensor system that a ATI Nano 17 force sensor and a solid-state TouchChip TCS1C Fingerprint Sensor (B)

The ATI Nano 17 sensor has been used in many studies as a standard instrument to measure fingertip force during grasping [1]. Its weight is around 9 grams with the size of 15 mm height and 17 mm diameter. Compared with the dimensions of the solid-state fingerprint sensor, the weight increase is not significant, considering in many studies those ATI Nano 17 sensors are mounted on aluminum plates. The solid-state fingerprint sensor is very thin and light weight, which doesn't affect the property of the force sensor as much. For most grasping studies that use the ATI Nano 17, the small dimension increase will not affect its usage. Even the optical fingerprint sensor is larger, it still could be useable in many applications.

Compared with high sampling rate of the force sensor, the current off-the-shelf fingerprint sensors have a very low sampling rate. However, as the contact position in the fingertip doesn't change very fast for many cases, the relative low sampling rate will unlikely pose a limitation of its use for typical grasping studies. For high temporal resolution requirement, a high speed fingerprint sensor could be used.

A Windows PC was used to collect the data from the force sensor and the fingerprint sensor. A Sensoray 626 data acquisition card reads the force data from the ATI Nano 17 force sensor at 1000 Hz sampling rate. A software was developed to read the ATI Nano 17 force sensor through a Sensoray 626 data acquisition card at 1000 Hz and the fingerprint image through a USB port at 10 fps. To ensure performance, the fingerprint images are processed with an image enhancement algorithm [8] to reduce noise and improve the clarity of the ridge and valley.

III. FINGERPRINT COORDINATE SYSTEM

To locate the contact area on a fingertip from a fingerprint, the entire fingerprint of the fingertip needs to be obtained and a coordinate system should be defined to uniquely represent the position of the fingerprint with a set of numbers. The curved surface of the fingertip can be represented on a flat 2D surface of a map with a continue mapping function. In this paper, a set of fingerprint images are taken and

stitched together to create a flatten fingerprint map that covers the entire fingertip. A coordinate system is defined on the fingerprint map.

A. Mosaicing Fingerprints

If a fingerprint sensor has a sufficient scanning window, a fingerprint map can be constructed from a sequence of fingerprints over a rolling fingertip on the fingerprint sensor. As the finger is rolled on the sensor, an image sequence over the rolling time can be acquired and stacked together without registration or alignment. If a fingerprint sensor has a small sensing area, only a small portion of the fingerprint can be captured at each time and the fingerprints between frames have to be aligned. Many techniques have been developed to combine multiple partially overlapping fingerprint images into a large fingerprint image [3]. Our setup has a sufficiently large fingerprint, and we instructed subjects to roll their fingertips on the fingerprint sensor without slippage, so that the images can be considered pre-aligned. A large fingerprint sensor can be used to build a fingerprint coordinate system and a small fingerprint sensor can be integrated with the force sensor to archive a compact setup.

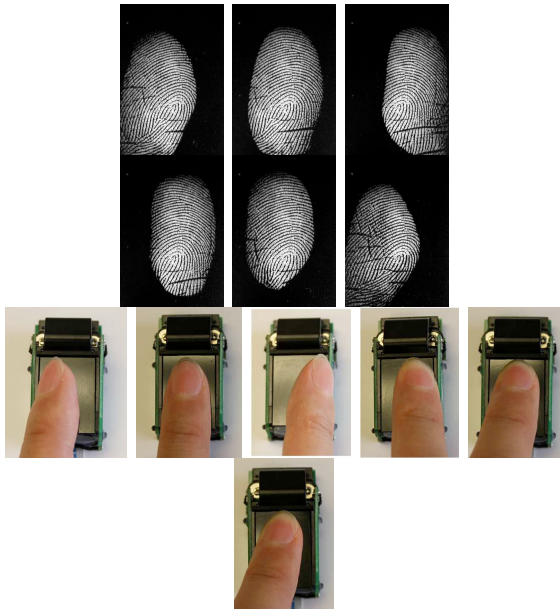


Fig. 4. A fingerpad is rolled on the fingerprint sensor, a set of fingerprint images are taken to construct a fingerprint map.

Figure 4 shows a fingerprint sequence captured during a fingerpad rolling of one subject. The fingerprint foregrounds are segmented from the background and then stacked together. The pixel values at overlapping areas are computed by averaging the pixel values of the overlapping foregrounds [18]. Figure 5 shows the composed fingerprint map from the fingerprint sequence in Figure 4-A. The enhancement algorithm proposed in Ref. [8] is used to remove noise and increase robustness. An enhanced fingerprint map is displayed in Figure 5-B.

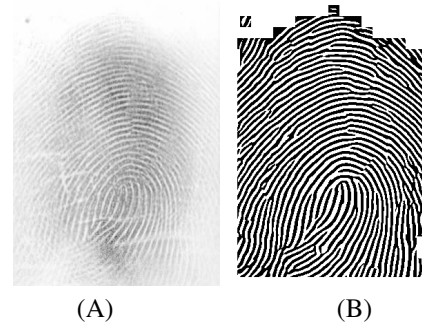


Fig. 5. (A) The fingerprint map merged from 200 fingerprint images; (B) The enhanced fingerprint map

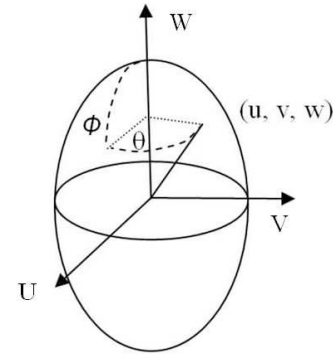


Fig. 6. A spherical coordinate system that is used to represent the contact position on the fingertip

B. Fingerprint Coordinate to Fingertip Coordinate Mapping

To express the contact position on the fingertip, a spherical coordinate is used. Considering that the shape of the fingerpad is very close to a quarter of ellipsoid, a point on the fingerprint can be represented with

$$\begin{aligned} u &= a \sin \phi \cos \theta \\ v &= b \sin \phi \sin \theta \\ w &= c \cos \phi. \end{aligned} \quad (1)$$

For each fingerpad, a , b , and c are fixed and the pair (θ, ϕ) can sufficiently represent any point on the fingerpad with $-\pi/2 < \theta < \pi/2$ and $0 < \phi < \pi/2$, as illustrated in Figure 6. ϕ is the colatitude, or zenith, and θ is the longitude, or azimuth. To further reduce the complexity, we assume the fingerpad is a spheroid, which indicates $a = b = r$ and a point on the fingertrip can be expressed as

$$\begin{aligned} u &= r \sin \phi \cos \theta \\ v &= r \sin \phi \sin \theta \\ w &= c \cos \phi. \end{aligned} \quad (2)$$

On the other hand, the contact position can be identified on the fingerprint map that is an unwrapped map of the fingerpad surface. We define the origin $(0, 0)$ of fingerprint map with the core point of the fingerprint, the x axis and the y axis along the short and long side of the fingerprint respectively as illustrated in Figure 7.

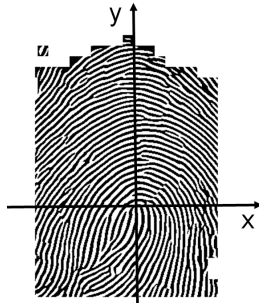


Fig. 7. The defined coordinate system on the fingerprint map

When we construct the fingerprint map, as the long side of the fingerprint sensor is aligned with the W axis in the fingertip coordinate (Figure 6), the rolling behavior on roll direction relates the angle θ to the latitude on the fingerprint map with

$$x = 2 \pi r \theta, \quad (3)$$

and the rolling behavior on the pitch direction related the colatitude angle ϕ_1 to the y axis in the fingerprint map with the elliptic integral of the second kind

$$y = c \int_0^{\phi_1} \sqrt{1 - \frac{c^2 - r^2}{c^2} \sin^2 \phi} d\phi, \quad (4)$$

as y is the length of the elliptical arc with ϕ_1 degree.

For a contact position (x, y) located in the fingerprint map, its θ and ϕ in the fingerpad coordinate system can be computed with Equations 3 and 4. The parameter c and r are calibrated with $\theta = 0$, $\theta = \pi/2$, $\phi = 0$, and $\phi = \pi/2$. Since it is very difficult to compute the colatitude angle ϕ_1 from an arc length of an ellipse, we retrieve the ϕ from a $\phi - y$ table pre-computed with numerical integration [6].

IV. CONTACT CHARACTERIZATION

When a fingertip contacts a force sensor, there are number of variables. Most research studies have only included the force and torque without considering the contact position or orientation on the force sensor or on the fingertip. With a fingerprint sensor, the FFPO sensor system can measure three additional contact characters: the contact position relative to the force sensor, the contact position on the fingertip, and the relative orientation between the force sensor and the fingertip.

A. Contact position Relative to the Force Sensor

Since the fingerprint sensor is rigidly attached to the force sensor and aligned as described in Section II, the contact area on the fingerprint sensor can be used to compute where the contact force is applied without assuming that it always goes through the origin or the contact area covers the whole sensor surface. For many human grasping studies, it is very important to know where exactly the contact is on the force sensor.

Figure 8-A shows a fingerprint image from the fingerprint sensor. The fingerprint area can be extracted from the background with image closing and erosion as shown in Figure 8-B. The centroid of the fingerprint area in the image can be computed and used as the contact position relative to the force sensor.



Fig. 8. (A) A fingerprint image. (B) The area of the fingerprint in the image.

B. Contact position and Orientation on the Fingertip

The fingerprint obtained with the fingerprint sensor can be registered onto the fingerprint map described in Section III-B with many different registration approaches [3]. Then the contact position and orientation on the fingerprint can be obtained from the registration result. However regular registration approaches require feature extraction and correlation matching that request a long computation time. In this paper, we utilize the fingerprint features, core point and local ridge orientation around the core point, to develop a simple approach to estimate the fingerprint position and orientation.

The core point in a fingerprint is defined as the point of maximum ridge line curvature. After fingerprint enhancement, an automatic core point extracting approach using a complex filter [13] is implemented and applied on the fingerprint image to obtain the position of the core point and its spatial orientation. As shown in Figure 9, the core point in the fingerprint map and an arbitrary fingerprint image is detected. For example the core point of the fingerprint map is at (167, 149) and core point of the arbitrary fingerprint is at (143, 111) from the left-bottom corner.

The local ridge orientation at a pixel is defined as the angle α of the fingerprint ridge at that point crossing through a small neighborhood centered at that pixel. Since fingerprint ridges are not directed, the direction angle α is defined in the range of $[0 \ 180]$. The simplest and most natural approach for extracting local ridge orientation is based on computation of gradients in the fingerprint image. As shown in Figure 10, the orientation around the core point in both the fingerprint map and the arbitrary fingerprint can be obtained. Their angle difference α can be computed as the rotation angle.

With the translation and rotation between the new fingerprint and fingerprint map, a point $p' = (x', y')$ in an arbitrary fingerprint image can be transformed to a point $p = (x, y)$ in the fingerprint map with

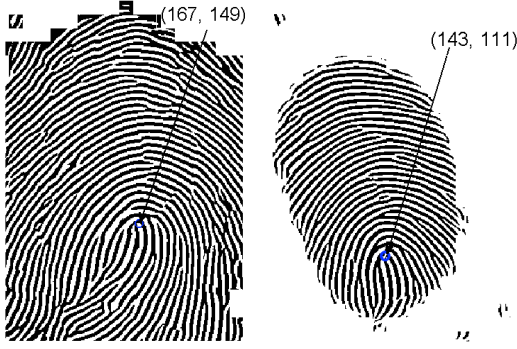


Fig. 9. The core point automatically detected with a complex-filter-based approach.



Fig. 10. The local ridge orientations around the core points.

$$(p - p'_{core}) = R(\alpha)(p' - p'_{core}) + (p'_{core} - p_{core}), \quad (5)$$

and

$$R(\alpha) = \begin{bmatrix} \cos(\alpha) & \sin(\alpha) \\ -\sin(\alpha) & \cos(\alpha) \end{bmatrix} \quad (6)$$

where p_{core} and p'_{core} are the core points of the fingerprint map and the arbitrary fingerprint respectively; α is the relative rotation angle between the fingerprint map and the arbitrary fingerprint. Now the center point of the arbitrary fingerprint can be registered to the fingerprint map with Equation 5. Then with Equation 3 and 4, the contact property can be fully characterized.

C. Contact Characterization

With the force sensor and the fingerprint sensor, not only the force and torque level but also the contact position relative to the force sensor, the contact position relative to the fingertip, and the relative orientation between the force sensor and the fingertip can be measured. A contact force between the human subject's fingerpad and the object in the world can be characterized in both the human subject's coordinate system and the world coordinate system.

The contact force (F_x, F_y, F_z) and torque (T_x, T_y, T_z) are not assumed to be always applied on the center of the force sensor. The fingerprint sensor measures the real contact position

(P_x, P_y, P_z) that is relative to the center of the force sensor and it is a variable during a grasping. The fingerprint sensor can also measure the contact position (ϕ, θ) and orientation α relative to the fingertip. Now the force (F_x, F_y, F_z) and torque (T_x, T_y, T_z) can be expressed in the human finger coordinate system.

V. EXPERIMENT RESULTS AND VERIFICATION

Three subjects have tested the new FFPO sensor. Subjects used their index fingers to press on the FFPO sensor system. The fingerprint sensor of the FFPO sensor collected the fingerprint image at 10 fps and the force sensor measured the force at 1000 Hz. With our software, it took roughly 30 seconds to build the fingerprint map and then the sensor is ready to measure the force/torque and the contact features. Subjects were asked to randomly place their fingertip on the fingerprint sensor and apply arbitrary force as they desired. As expected, the force sensor reading is not affected by the fingerprint sensor after initial force sensor offset calibration. The current software can estimate the contact position and orientation within one second for each fingerprint. The main computation time is consumed by the core point localization and it depends on the resolution of the images and the precision requirement.

Totally 1500 fingerprint images were collected. Because the ground truth about the positions of the core points in the fingerprint images were not known and it would be a tedious task to manually find the core points and record their positions in all the images, we randomly selected 100 fingerprint images out of 1500 images to estimate the accuracy. The core points in those images were manually labeled and their x and y pixel positions were recorded and compared with the results of the core point localization approach we used. We found that the average error was within 6 pixels and the fingerprint sensor has 500 dpi, so on average, the error was within 6/500 inches that was 0.3 mm.

There are several factors that could affect the resolution of the fingerprint registration result. Among them, the most important ones are the resolution of the fingerprint sensor and the feature of ridges and valleys in the fingerprint which are different between human subjects. The resolution of the fingerprint sensor directly affects the resolution of the finger contact resolution. However, since the computation time of core point localization approach is correlated with the fingerprint resolution, it is a trade-off between the spatial and temporal resolutions.

VI. DISCUSSION AND FUTURE WORK

This paper proposed a novel fingertip force and position measurement apparatus, FFPO sensor, that can measure the contact position and orientation on the force sensor and the fingertip, as well as the contact force. In many grasping or manipulation studies, with this device, not only the contact force but also the contact spatial features on both the fingerpad and the sensor can be obtained without sacrificing any precision or dimension. It allows roboticists

and neuroscientists to characterize human hand locomotions in more detail.

In this paper, the contact position relative to the sensor is obtained with the centroid of the fingerprint region, and the contact position and orientation relative to the fingertip is obtained with the registration from the fingerprint reading to the prebuilt fingerprint map. Three subjects has used this FFPO sensor. They all reported that the device was easy to use. Compared with traditional force sensors, the FFPO sensor requires extra roughly 30 seconds to build the fingerprint map and the position reading sample rate is currently around 10 Hz. Compared with tactile sensors, the FFPO sensor provides full 6-axis force/torque reading with high precision, which usually is a luxury to ask for a tactile sensor.

Currently, we detect the core point and the local orientation around the core point to estimate the registration transformation from an arbitrary fingerprint to the fingerprint map. There are other minutiae points that can be used for the registration purpose with the core point is not in the view of the fingerprint sensor. Other general correlation-based registration algorithms can also be used. Since the speed of the registration computation is usually related to the resolution of the images, it is a trade-off between the contact spatial resolution in the measurement and temporal resolution.

In the future, we plan to build a 3D fingerprint map to remove the assumption that a fingertip has an ellipsoid shape. It will allow a fingerprint to be directly registered on the 3D fingerprint map and a more precise contact position can be obtained. We also plan to carry out a larger experiment to include more subjects to better characterize the precision and resolution of this new device. We will develop new experimental approaches to validate the sensor system with actual known contact spatial features.

In addition, the fingerprint sensor also allow us to measure the contact area which is correlated to the contact force and the tissue compliance feature, which is an important study itself [14]. Our current work doesn't include the skin plasticity and consider the fingerprint image as non-distorted by assuming that the contact force is normal (orthogonal to the fingerprint surface) and the user doesn't apply traction or torsion. However when we study varieties of fingertip forces including shear force, this assumption may not hold for many cases. In the future, we plan to include the skin plasticity in consideration and use the deformation in the fingerprint to help us to model tissue features and provide more detailed information about the fingerpad contact features in a grasping and manipulation. It would be a very useful tool for studies in robotics, haptics, and neuroscience.

VII. ACKNOWLEDGMENTS

This research was supported by the University of South Florida Seed Grant.

REFERENCES

- [1] G. Baud-Bovy and J.F. Soechting. Factors influencing variability in load forces in a tripod grasp. *Exp. Brain Res.*, 143:57–66, 2002.
- [2] Ingvars Birznieks, Per Jenmalm, Antony W. Goodwin, , and Roland S. Johansson. Encoding of direction of fingertip forces by human tactile afferents. *Journal of Neuroscience*, 21:8222–8237, 2001.
- [3] L.G. Brown. Image registration techniques. *ACM Computing Surveys*, 24(4):326376, 1992.
- [4] A. A. Cole, P. Hsu, and S.S. Sastry. Dynamic control of sliding by robot hands for regrasping. *IEEE Trans Robotics and Automation*, 8:42–52, 1992.
- [5] M.R. Cutkosky. On grasp choice, grasp models, and the design of hands for manufacturing tasks. *IEEE Trans Robotics and Automation*, 5:269–279, 1989.
- [6] H. B. Dwight. *Tables of Integrals and Other Mathematical Data*. The Macmillan Co., 4th ed. edition, 1961.
- [7] Jonathan Engel, Jack Chen, and Chang Liu. Development of polyimide flexible tactile sensor skin. *Journal of Micromechanics and Microengineering*, 13:359–366, 2003.
- [8] L. Hong, Y. Wan, and A. K. Jain. Fingerprint image enhancement: Algorithm and performance evaluation. *IEEE Transactions on Pattern Analysis and Machine Intelligence*, 20:777–789, 1998.
- [9] T. Iberall. Human prehension and dextrous robot hands. *Intl J Robotics Research*, 16:285–299, 1997.
- [10] R. S. Johansson and G. Westling. Roles of glabrous skin receptors and sensorimotor memory in automatic control of precision grip when lifting rougher or more slippery objects. *Exp Brain Res*, pages 550–564, 1984.
- [11] V. Levesque and V. Hayward. Experimental evidence of lateral skin strain during tactile exploration. In *Proc. Eurohaptics*, pages 1–13, 2003.
- [12] J.R. Napier. The prehensile movements of the human hand. *Journal of Bone Joint Surg*, 38B:902–913, 1956.
- [13] K. Nilsson and J. Bigun. Localization of corresponding points in fingerprints by complex filtering. *Pattern Recognition Letters*, 24:2135–2144, 2003.
- [14] D.T.V. Pawluk and R.D. Howe. Dynamic contact mechanics of the human fingerpad against a flat surface. *ASME J. Biomechanical Engineering*, 121:178–183, 1999.
- [15] Inc. Pressure Profile Systems. www.pressureprofile.com.
- [16] M.P. Rearick, A. Casares, and M. Santello. Task-dependent modulation of multi-digit force coordination patterns. *J. Neurophysiol.*, 89:1317–1326, 2003.
- [17] D. Rempel, E. Serina, and E. Klinenberg et al. The effect of keyboard keyswitch make force on applied force and finger flexor muscle activity. *Ergonomics*, 40(8):800808, 1997.
- [18] Bolle R.M., N.K. Ratha, and J.H. Connell. Image mosaicing for rolled fingerprint construction. In *ICPR*, pages 1651–1653, 1998.
- [19] M. Santello and J. F. Soechting. Force synergies for multifingered grasping. *Exp. Brain Res.*, 133:457–467, 2000.
- [20] J. K. Shim, M. L. Latash, and V. M. Zatsiorsky. Prehension synergies: trial-to-trial variability and hierarchical organization of stable performance. *Exp. Brain Res.*, 152:173–184, 2003.
- [21] J. K. Shim, M. L. Latash, and V. M. Zatsiorsky. Prehension synergies in three dimentions. *J. Neurophysiol*, 93:766–776, 2005.
- [22] C.L. Taylor and R.J. Schwartz. The anatomy and mechanics of the human hand. *Artificial Limbs*, 2:22–35, 1955.
- [23] Inc. Tekscan. www.tekscan.com.
- [24] Inc. Upek. www.upek.com/solutions/government/sensor.asp.
- [25] G. Westling and R.S. Johansson. Responses in glabrous skin mechanoreceptors during precision grip in humans. *Exp. Brain Res.*, 66:128–140, 1987.
- [26] Kurita Y, Ikeda A., Ueda J., and Ogasawara T. A fingerprint pointing device utilizing the deformation of the fingertip during the incipient slip. *IEEE Transactions on Robotics*, 21:801– 811, 2005.